A Unique Cytoskeleton Associated with Crawling in the Amoeboid Sperm of the Nematode, *Ascaris suum*

Sol Sepsenwol,* Hans Ris,‡ and Thomas M. Roberts§

* Department of Biology, University of Wisconsin-Stevens Point, Stevens Point, Wisconsin 54481;
‡ Department of Zoology and Madison Integrated Microscopy Resource, University of Wisconsin, Madison, Wisconsin 53706; and
§ Department of Biological Science, Florida State University, Tallahassee, Florida 32306

Abstract. Nematode sperm extend pseudopods and pull themselves over substrates. They lack an axoneme or the actin and myosins of other types of motile cells, but their pseudopods contain abundant major sperm protein (MSP), a family of 14-kD polypeptides found exclusively in male gametes. Using high voltage electron microscopy, a unique cytoskeleton was discovered in the pseudopod of in vitro-activated, crawling sperm of the pig intestinal nematode *Ascaris suum*. It consists of 5–10-nm fuzzy fibers organized into 150–250-nm-thick fiber complexes, which connect to each of the moving pseudopodial membrane projections, villipodia, which in turn make contact with the substrate. Individual fibers in a complex splay out radially from its axis in all directions. The centripetal ends intercalate with fibers from other complexes or terminate in a thickened layer just beneath the pseudopod membrane. Monoclonal antibodies directed against MSP heavily label the fiber complexes as well as individual pseudopodial filaments throughout their length. This represents the first evidence that MSP may be the major filament protein in the *Ascaris* sperm cytoskeleton. The large fiber complexes can be seen clearly in the pseudopods of live, crawling sperm by computer-enhanced video, differential-interference contrast microscopy, forming with the villipodia at the leading edge of the sperm pseudopod. Even before the pseudopod attaches, the entire cytoskeleton and villipodia move continuously rearwards in unison toward the cell body. During crawling, complexes and villipodia in the pseudopod recede at the same speed as the spermatozoon moves forward, both disappearing at the pseudopod–cell body junction. Sections at this region of high membrane turnover reveal a band of densely packed smooth vesicles with round and tubular profiles, some of which are associated with the pseudopod plasma membrane. The exceptional anatomy, biochemistry, and phenomenology of *Ascaris* sperm locomotion permit direct study of the involvement of the cytoskeleton in amoeboid motility.

Ameboid motility, generally defined as the crawling of cells over a substrate by means of pseudopods, is observed throughout the animal kingdom.[1] Two types of force-generating systems have been proposed to explain this kind of motility in diverse cells: a cytoskeleton-based system and a membrane flow-based system. In the former, cytoplasmic actin–myosin interactions reminiscent of the model for vertebrate skeletal muscle are required for locomotion (see reviews by Clarke and Spudich, 1977; Pollard, 1981, 1986; Trinkhaus, 1984). In membrane-based models, the attachment and flow of membrane generate the necessary forces (see Ishihara et al., 1988). In this study we present a novel example, the crawling sperm of the nematode *Ascaris suum*, in which both cytoskeleton and membrane flow are involved in its locomotion. The cells are unusual because they contain only traces of actin (<0.5%), tubulin (one centriole), and no myosin (Nelson and Ward, 1981; reviewed by Roberts et al., 1989), yet crawl by means of a pseudopod at >70 μm/min on glass (Sepsenwol, S., and S. J. Taft, manuscript submitted for publication). The gamete's most abundant protein is the 14-kD major sperm protein (MSP)[2] (Klass and Hirsh, 1981; Nelson and Ward, 1981). In the activated spermatozoon of the nematode *Caenorhabditis elegans*, MSP is localized in the pseudopod (Ward and Klass, 1982). When the pseudopods of nematode sperm are examined in thin section by conventional transmission electron microscopy, they appear to contain unorganized masses of filaments as thin as 2 nm in diameter (Roberts et al., 1989; Foor et al., 1971; Foor, 1974; Wright and Sommerville, 1984, 1985; Burghardt and Foor, 1978; Abbas and Cain, 1984). By examining

1. Ameboid movement is used here to describe any locomotion by which a cell crawls over a substrate. Some features of nematode sperm locomotion are quite different from those described in other crawling cells.

2. *Abbreviations used in this paper:* DIC, differential-interference contrast; HVEM, high voltage electron microscopy; MSP; major sperm protein.

whole mounts and semithick sections by high voltage electron microscopy (HVEM), however, we have discovered in the pseudopod of *Ascaris* sperm an elaborate, dynamic system of interconnected thin filaments which are organized into large units, the fiber complexes. The complexes can be visualized in living cells without staining or labeling, and their behavior in motile cells studied in real-time.

The structure and composition of filaments that form the complexes have been examined by immunolabeling at the light and electron microscopic levels. Entire fiber complexes as well as individual fibers fixed in situ label strongly with antibodies against MSP, indicating that this protein is a major constituent of the *Ascaris* sperm pseudopod cytoskeleton.

Materials and Methods

Unless otherwise specified, all biochemical reagents were purchased from Sigma Chemical Co. (St. Louis, MO).

Collection of Ascaris

Male *Ascaris* worms were expressed from the small intestine of freshly killed pigs, rinsed, and transported in PBS (0.15 M NaCl, 7.5 mM $MgCl_2$, 1.5 mM $CaCl_2$ in 0.1 M phosphate, pH 7.2–7.4) at 37–41°C. Worms were maintained in the laboratory in PBS gassed with 15% CO_2 in N_2.

Vas Deferens Extract

An ultrafiltrate (0.2-μm pore size) of a 25,000 *g* supernatant of an homogenate of the glandular male vas deferens was prepared as described in Sepsenwol et al. (1986).

Sperm Preparation for Electron Microscopy

The contents of the seminal vesicle from one adult male (~10^7 spermatids) was emptied into 8–15 ml 0.15 M NaCl in 20 mM Hepes, pH 7.2 (Hepes-saline buffer), preheated to 40°C, and gassed with 15% CO_2/N_2.

Whole Mounts. 30 μl of vas deferens extract were added to 6 ml spermatid suspension in a 60-mm plastic dish containing acid-washed glass coverslips and 150-mesh gold grids which had been formvar-carbon-coated and made hydrophilic by glow discharge. The dish was transferred to a 40°C incubator and gassed with 15% CO_2 in N_2 throughout incubation and fixation. After 15–20 min, cells were fixed at room temperature for 30 min with one of three fixatives: 2.5% glutaraldehyde, 0.05% saponin, 0.2% tannic acid in 0.1 M Hepes buffer, pH 7.4 (Maupin and Pollard, 1983); or 2.5% glutaraldehyde, 0.1% Triton X-100 in Hepes buffer; or 2.5% glutaraldehyde, 4% paraformaldehyde in Hepes buffer. Grids and coverslips were rinsed and stored in Hepes buffer at 4°C. Washed grids were postfixed in 0.1% aqueous OsO_4 for 10 min and stained with 1% aqueous uranyl acetate for 10 min. After dehydration in ethanol, grids and coverslips were critical point dried without intermediate solvent, using filter dried, liquid CO_2 (Ris, 1985).

Semithick Sections. For plastic embedment spermatid suspensions were activated in polypropylene test tubes, fixed with glutaraldehyde–saponin–tannic acid fixative for 30 min, washed in buffer, pelleted at 1,000 *g*, postfixed in 0.1% OsO_4 for 10 min, rinsed in distilled H_2O, and stained with 1% aqueous uranyl acetate. Fragments of pellets were dehydrated in graded ethanols and embedded in Epon–Araldite. Semithick sections (0.12–0.25 μm) were mounted on Formvar-coated grids, stained with 7.5% aqueous uranyl magnesium acetate at 50°C for 2 h followed by 20 min in lead citrate, then lightly coated with carbon.

Scanning Electron Microscopy

Critical point dried cells on coverslips were ion beam sputter coated with a thin layer of platinum and examined with a low voltage scanning electron microscope (model S-900; Hitachi Ltd., Tokyo) operating at 2 kV.

High Voltage Electron Microscopy (HVEM)

Electron micrographs of whole mounts and semithick sections were prepared at 1 MV with the AEI EM7 HVEM at the Madison Integrated Microscopy Resource.

Enhanced Video Differential-Interference Contrast (DIC) Microscopy

Crawling cells activated as above were observed on a Universal microscope (Carl Zeiss, Inc., Thornwood, NY) with Nomarski DIC optics using a Zeiss 63× plan apochromat objective and a Sierra Scientific (Mountain View, CA) LSN-1 Newvicon video camera. The video signal was processed directly with a (model 9200EX; Quantex, Sunnyvale, CA) real-time image-processing system. An out of focus image was stored and digitally subtracted from a frame-averaged image to reduce background. Image contrast was enhanced and processed images were recorded on a Sony (model 5800) 3/4 inch videotape recorder, then played back through the Quantex system to freeze individual frames. Frames were photographed directly from the screen of a Conrac high-resolution black and white monitor onto Panatomic-X black and white film (Eastman Kodak Co., Rochester, NY). (A preliminary report on imaging techniques used to study *Ascaris* sperm appears in a presentation summary by Pawley et al., 1986.)

Crude MSP Immunogen Protein Preparation

Spermatids from 25–50 males were frozen at −70°C, thawed, glass homogenized, and the crude debris was pelleted at 1,000 *g*. The supernate was centrifuged at 100,000 *g* 30 min at 4°C. The resultant supernate was dialyzed against 50 mM acetate buffer, pH 4.5, at 4°C overnight. Acid-precipitatable material was removed by centrifugation and the final supernate, designated AS-S100, was concentrated by vacuum dialysis against PKM buffer (20 mM Pipes, 25 mM KCl, 1 mM $MgCl_2$, pH 7.6).

Monoclonal Antibodies

Antibodies against MSP were generated by standard hybridoma procedures using AS-S100 *Ascaris* sperm protein fraction (above) as immunogen in Balb/c mice. Antibody was purified from mouse ascites fluid by affinity chromatography against immobilized anti-mouse IgG (Cappel Laboratories, Cochranville, PA). Their antigen recognition patterns were tested by immunoblotting against AS-S100, separated on a 10–20% gradient polyacrylamide gel (Laemmli, 1970), and electrophoretically transferred to nitrocellulose (Towbin et al., 1979; as modified by Ward et al., 1986). Antibody-labeled bands were visualized using horseradish peroxidase-conjugated anti-mouse IgG (Jackson Immunoresearch Laboratories, Inc., Avondale, PA), followed by 4-chloro-1-naphthol reagent.

Cell Labeling for Light Microscopy

Activated sperm were pipetted onto glass coverslips, allowed to settle 5–10 min, and fixed 30 min in 2% glutaraldehyde, 0.5% Triton X-100 in PKM buffer. Cells were washed in buffer, treated three times for 10 min with 10 mM $NaBH_4$ in PKM buffer, washed in PKM buffer, and incubated with anti-MSP antibody (20–30 μg/ml) in PKM buffer for 2 h. After a 15-min wash in buffer, the cells were incubated in FITC-conjugated anti-mouse IgG (Cappel Laboratories), washed, and examined under a Zeiss standard microscope with epifluorescent illumination.

Cells were stained with phalloidin as follows: sperm were fixed in glutaraldehyde-Triton X-100 as above, blocked with borohydride, incubated 30 min with rhodamine-conjugated phalloidin (Molecular Probes, Inc., Junction City, OR) at 4 μg/ml in PKM buffer, washed in PKM buffer, and examined as above. A primary culture of mouse peritoneal fibroblasts, grown for 6–7 d in RPMI medium on sterile coverslips, was fixed and labeled as above, and used as a positive F-actin control.

Cell Labeling for Electron Microscopy

5-nm colloidal gold particles prepared by the tannic acid–citrate method (Slot and Geuze, 1985) were conjugated to affinity-purified anti-MSP antibody as previously described (Roberts et al., 1986); gold-antibody was diluted to a light pink in PKM buffer. Sperm were prepared and labeled as above, incubating with the gold-antibody for 2 h. Labeled cells were washed in buffer, postfixed 30 min in 0.1% OsO_4 in PKM buffer, washed in distilled H_2O, dehydrated in graded ethanols to propylene oxide, and embedded in Polybed 812 (Polysciences, Inc., Warrington, PA). Thin sections were mounted on Formvar-carbon-coated copper grids, stained with

uranyl acetate and lead citrate, and examined with a transmission electron microscope (model 100CX; JEOL USA, Peabody, MA) at 80 kV.

Results

General Morphology and Surface Features of the Pseudopod

Fig. 1 is a scanning electron micrograph of an activated *Ascaris* spermatozoon attached to glass. It is the largest reported among the nematodes; in vitro–activated, motile sperm possess an hemispherical cell body 10–12 μm in diameter positioned above a pseudopod extending up to 15 μm beyond the cell body. *Ascaris* sperm are permanently and distinctly bipolar. When examined in sections of sperm fixed in situ, the cell body contains all of the cell's membrane-bound organelles: mitochondria, condensed nucleus, a large refringent body, and numerous membranous organelles which fuse with the cell membrane during activation. The pseudopod contains filaments. The membrane over the cell body has no protrusions and contains numerous pits where the membranous organelles have fused with it. The pseudopod membrane, on the other hand, has no pits, but many finger-like projections, the villipodia,[3] which cover the pseudopod from tip to base. On the ventral surface, the villipodia are flattened where they come into contact with the substrate. These membrane specializations can be observed in living cells with phase-contrast and DIC optics. They form continuously at the tip of the pseudopod, move rapidly rearwards over the surface and disappear at the junction of pseudopod and cell body. In Fig. 1, two villipodia can be seen tucking under an infolding, or lip, where the cell body and pseudopod membranes meet. About 20 min after activation in vitro, these moving villipodia form broad areas of attachment to the substrate and pull the cell body along as they move rearwards beneath the pseudopod. The cells crawl at a rate identical to the movement of the villipodia (25–75 μm/min on glass).

The Pseudopod Cytoskeleton: Fiber Complexes

Cells were activated on electron microscopy grids and fixed with glutaraldehyde in the presence of the nonionic detergent, Triton X-100. This fixative prevents rapid changes in overall cell morphology. The detergent removes the pseudopod membrane, revealing its fibrous cytoskeleton. The plasma membrane over the cell body does not solubilize under these conditions. The cells and exposed cytoskeleton were examined whole with HVEM. Fig. 2 is a low magnification stereo view showing the entire cell.[4] The thick cell body is electron opaque. The pseudopod, however, contains a striking array of 150–250-nm-wide branched assemblages, the fiber complexes, made up of much smaller fibers. The complexes extend from the leading edge through the length of the pseudopod and stop at the pseudopod–cell body junction. Each branch of the complex terminates in finger-like

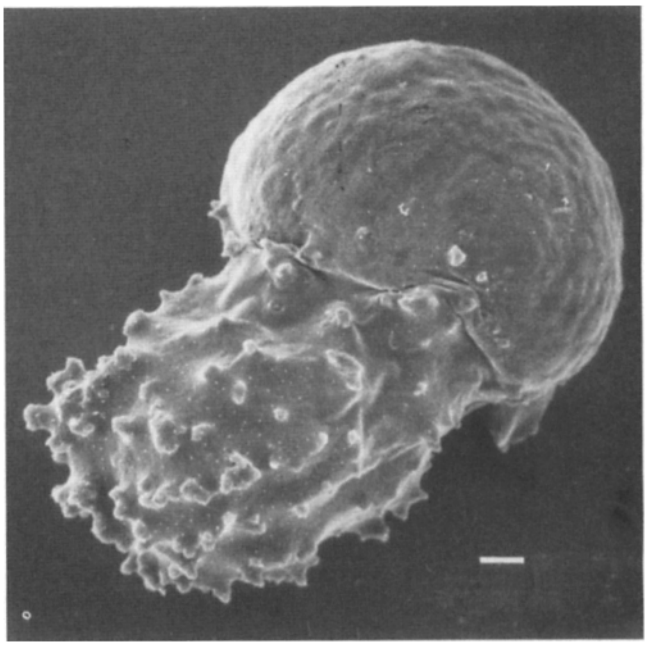

Figure 1. Scanning electron micrograph of *Ascaris* spermatozoon 17 min after in vitro activation on glass. Glutaraldehyde–saponin fixation. Bar, 1 μm; V_{accel}, 2 kV.

projections of fibers congruent with the villipodia which arise at the leading edge and cover the surface of the pseudopod. In stereo, it can be seen that some complexes along the base of the pseudopod branch vertically and end in villipodia on the dorsal surface. In sperm that are not attached to substrate, the pseudopod is more cylindrical with a blunted tip. Its complexes fill the entire volume, generating villipodia at the tip which move rearwards over the entire surface of the pseudopod membrane. When attached, the pseudopod is more flattened and complexes spread out mainly, but not exclusively, along the attached plane of the pseudopod. In crawling cells, complexes form a continuous mat of fibers along the base of the pseudopod (see Fig. 2), or send projections 1 or 2 μm into the upper pseudopod membrane to form nonadherent villipodia.

In the stereo micrograph, Fig. 3, some complexes are shown at higher magnification in a more dispersed state. They consist of nonuniform or "fuzzy" fibers whose overall diameter in whole mounts ranges from 5 to 10 nm. The arrangement of the fibers in complexes varies; some of them are oriented parallel to and concentrate about a central core of the complex (Fig. 3, *small arrow*). Most fibers splay out radially from the core (Fig. 3, *large arrowhead*), at an angle of 10–90° to its axis and tipped toward the forward end of the cell. As also seen in Fig. 2, the radial fibers interweave with those from adjacent complexes with one end always anchored in a complex. The fiber complexes are thus interconnected into one continuous unit filling the entire pseudopod. The tips of the complexes, normally much more dispersed when associated with intact membrane, are collapsed in whole-mounted, detergent-treated sperm (compare to Fig. 5). Fig. 4 is a semithick cross section through several fiber complexes and illustrates the amorphous dense 20-nm cores which identify individual complexes and the aster of fibers

3. While the moving membrane specializations in *Ascaris* sperm resemble microvilli, they are generally stubbier and are not associated with actin filaments. The term "filipodia" used by others does not seem appropriate to describe short stubby projections, hence, "villipodia."

4. Stereo figures should be viewed with a standard 2× stereo print viewer.

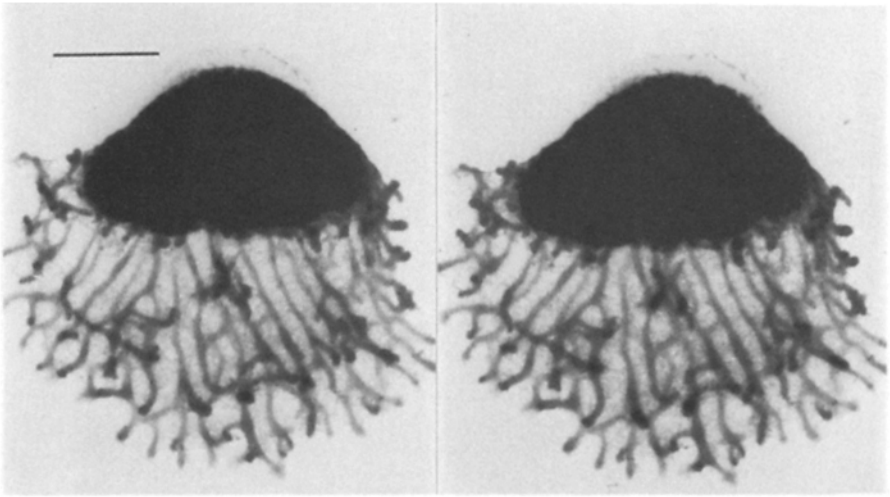

Figure 2. Low power stereo electron micrograph of whole mount of *Ascaris* spermatozoon prepared with glutaraldehyde–Triton X-100 detergent fixative. Note how numerous fiber complexes branch and terminate in villipodia, arising over the upper and lower surfaces of the pseudopod. The spaces between complexes are filled with splayed fibers. The region in which the complexes terminate is obscured by the electron-dense cell body, which contains the nucleus, mitochondria, membranous organelles, and refringent granules. 15–20 complexes are in close apposition to the cell body. Bar, 5 μm; V_{accel}, 1 MV.

radiating from them. The cores do not appear to be separate structures but common attachment points of the ends of several individual fibers. The dense varicosities are cross sections of fibers. In cells allowed to become aerobic, the terminal branches of all but a few of the complexes and their villipodia disappear. The remaining complexes become rigid and rodlike with densely packed fibers all oriented parallel to the long axis of the complexes (not shown). These rigid complexes form long spikes instead of villipodia and move side to side, but there is no evidence of rearward membrane flow. This and Fig. 3 suggest that the fibers in complexes of crawling sperm are able to splay out much like the ribs of an umbrella and, in similar fashion, tend to collapse to a position parallel to the axis of the complex. Fig. 5 *a* is a longitudinal semithick section of a fiber complex as it ends in a villipodium. The fibers inside each villipodium are more highly dispersed than the rest of the complex, emerging in all directions toward the villipodial membrane. In the villipodium, the radiating filaments appear to make numerous contacts with the electron-opaque region apposed to the inner layer of the plasma membrane (Fig. 5 *b*, *arrow*). The dense submembrane layer is a constant feature over both the pseudopod and cell body, as is the fibrous material on the outer surface. Where the membrane is cut perpendicularly, the dense lamina apposed to the inner face of the cell membrane appears as a "carpet" of fibrillar material (Fig. 5 *a*, *bracket*).

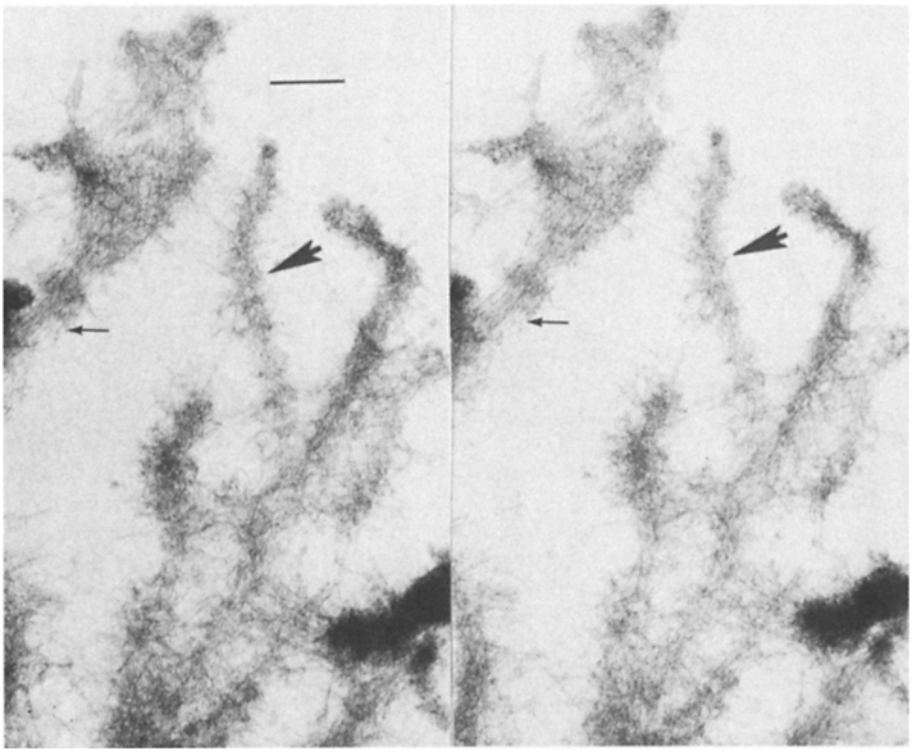

Figure 3. Stereo electron micrographs of spermatozoon whole mount prepared with glutaraldehyde–Triton X-100 fixative. A more highly dispersed preparation compared to Fig. 2; the individual complexes and their terminations are clearly distinguished. The configurations of fibers in relation to the complex are shown; fibers normally are splayed out radially from the center of the complex (*large arrowhead*). In aging cells, fibers can collapse close to the core of the complex into parallel bundles (*small arrow*). Bar, 0.5 μm; V_{accel}, 1 MV.

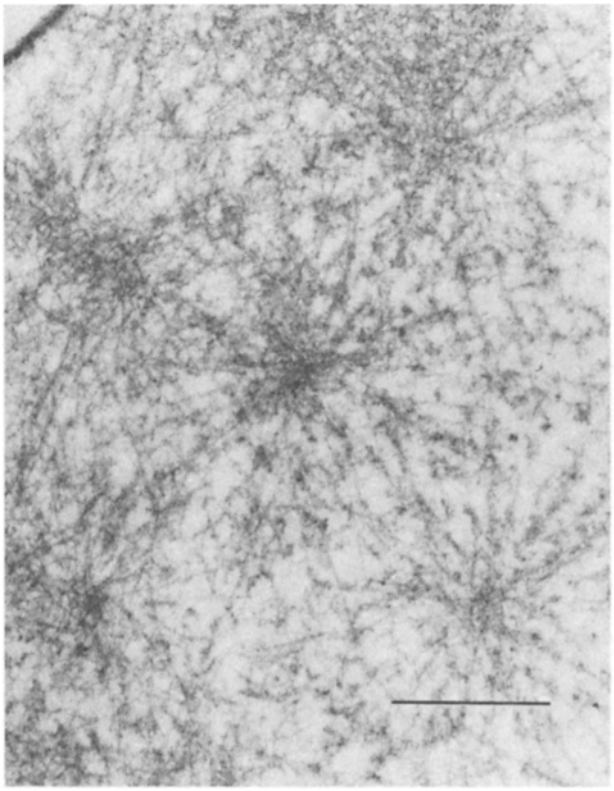

Figure 4. Electron micrograph of semithick cross section of fiber complexes in spermatozoon pseudopod prepared with glutaraldehyde–tannic acid–saponin fixative. "Fuzzy" fibers radiate from cores of several complexes. The parallel fibers at the cores of the complexes are seen as punctate structures along the radial filaments. Bar, 1 μm; V_{accel}, 1 MV.

Villipodia and Fiber Complex Translocation in Live Sperm

Many of the features of fiber complexes in the pseudopod, how they form and move, can be clearly observed in living fully activated *Ascaris* sperm using the higher resolution and contrast of computer-enhanced video DIC. Fig. 6 is a time-lapse sequence of enhanced video DIC images of a motile spermatozoon on glass. The cell in this sequence is activated and its pseudopod is flattened but not attached (i.e., not crawling) so that the relative movement of structures in the pseudopod can be easily followed at high magnification. The fiber complexes appear as large, refringent fibers 0.2–0.3 μm in diameter. They can be seen as early as 6 min into activation, before the pseudopod is fully extended and attached. The unusual behavior of the cytoskeletal complexes is shown in the low power sequence (Fig. 6, *a–c*). A group of five branched refringent fibers oriented roughly parallel to the cell's long axis is identified in Fig. 6 *b* and located ~10 s later in Fig. 6 *c*; the entire array moves as a unit toward the rear of the pseudopod (rate, ~25 μm/min). At the same time, a group of villipodia can be seen above and to the left of the area (Fig. 6, *asterisk*) moving the same distance as the group of complexes. The overall length of the pseudopod remains constant. A sequence of images at higher magnification (Fig. 6, *d–g*) shows the continuous formation of individual villipodia at the leading edge in association with fiber complexes.

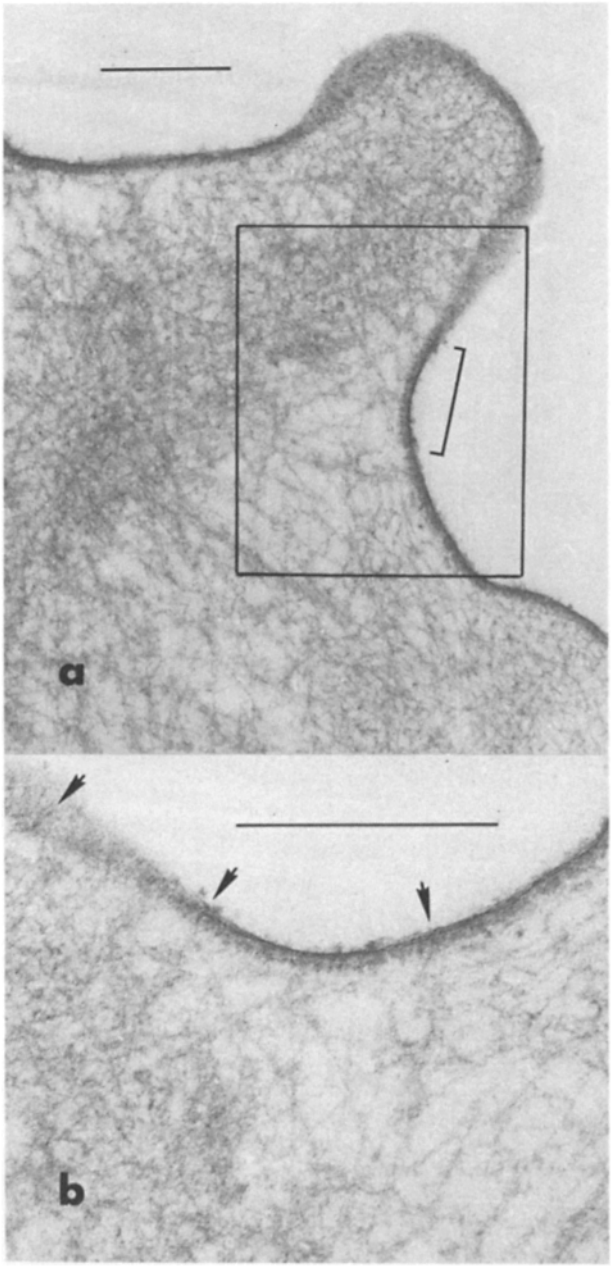

Figure 5. Semithick section of a villipodium, associated fiber complex, and specialized plasma membrane in glutaraldehyde–tannic acid–saponin fixative. (*a*) Fiber complex shown in longitudinal section as it enters villipodium. Individual fibers have the same fuzzy appearance in section as in whole mount preparation shown in Fig. 3. Inside the villipodium, fibers are more loosely bundled than in the bottle-brush branches of the complex. The small fibers radiate in all directions toward a dense layer apposed to the inner lamina of plasma membrane. The layer is a feature of both pseudopod and cell body membranes. In some cross sections of the membrane, the layer resembles a carpet of closely packed fibrils (*bracket*). (*b*) Enlargement of area in *a*; the specialized plasma membrane. Fibers from complexes make many contacts with the dense layer within the villipodium (*small arrows*). The irregular fibrous material on the outer layer of the plasma membrane does not appear to be continuous with the submembrane material. Bars, 0.5 μm; V_{accel}, 1 MV.

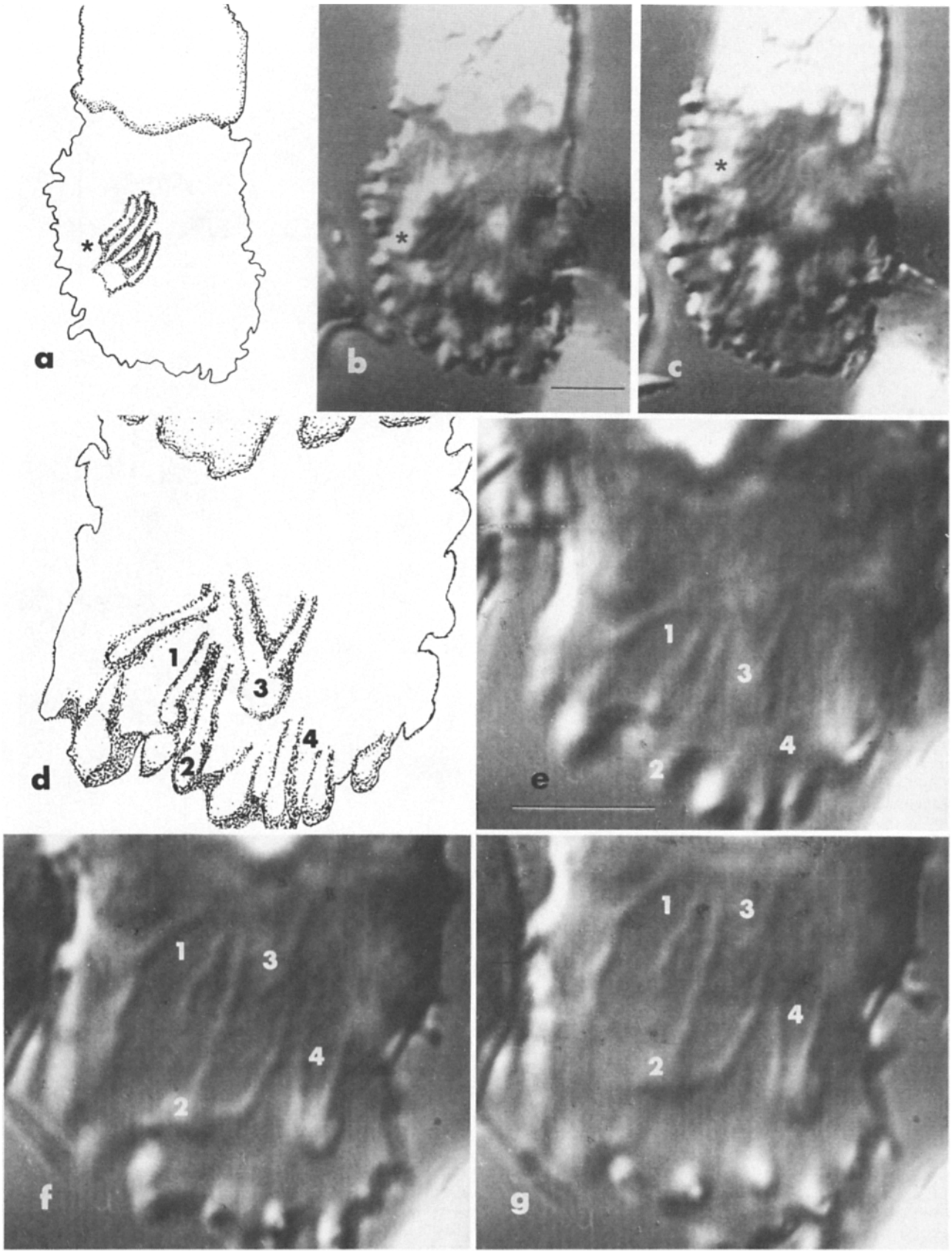

Figure 6. Time lapse, video-enhanced, DIC images of living, in vitro-activated *Ascaris* spermatozoa on glass; contrast-enhanced, background-subtracted, four-frame (1/15 sec) averaged image shown. (*a–c*) Low magnification sequence, showing overall bipolar morphology of a fully motile cell with its extended pseudopod and large refractile cell body. (*a*) One set of fiber complexes in *b* (*) is drawn for clarity in the first panel. (*c*) The same cell 10 s after *b*, showing the same set of complexes after it has migrated near the junction of pseudopod and cell body. Their relative positions are unchanged. (*d–g*) Higher magnification sequence showing the association of fiber complexes with villipodia at feature *1*, *2*, and *3* as they progress rearward and a new villipodium formed at feature *4*. *d* is a drawing of representative features found in *e*. Feature *1* can be seen in *g* disappearing at the cell body–pseudopod junction. *f* follows *e* by ~10 s; *g* follows *f* by ~3 s. Bars, 5 μm.

The complexes may branch as they are formed, migrate rearward toward the cell body, and disappear at the cell body–pseudopod junction. At Fig. 6 *d*, position 2, a villipodium forms at the leading edge from a previously assembled fiber complex and both migrate rearwards in succeeding frames. Some of the branches appear to join (see position 2 in Fig. 6, *f* and *g*), but HVEM whole mounts show that villipodia form on only one of the apposing complexes (Fig. 2). In all cases examined, the entire assembly of fibers moves rearward as a unit in concert with the villipodia. Once assembled at the leading edge, the interconnected fiber complexes form a semirigid framework which does not change shape. When a cell turns, new branched complexes are formed to the side of the turn, established complexes maintain the same relative positions, and the cell body is pulled around in the new direction. The movement of fiber assemblies occurs in activated cells whether or not they are attached to the substrate (i.e., crawling) and is always associated with rapid retrograde membrane flow.

Both villipodia and fiber complexes disappear at the "lip" formed by the cell body where it joins the base of the pseudopod. Fig. 7 shows semithick sections of this region. In Fig. 7 *a*, the complexes are not tethered to any obvious structures within the cell body. There is, however, a dense aggregation of smooth membrane vesicles just inside the cell body, packed around the mitochondria and membranous organelles at the junction (Fig. 7 *a*, *dotted line*). Farther into the cell body, the vesicles are more dispersed. At higher magnification (Fig. 7 *b*), most vesicle profiles within the band are round, but unusual tubular or flattened forms are also seen. Toward the center of the junction of pseudopod and cell body, the tubular vesicles are oriented with their long axes parallel to the plane of the junction. Those apposed and near to the plasma membrane are aligned parallel to it. Because of the submembrane dense layer, it is not possible to determine if there are vesicles continuous with the plasma membrane itself. In some sections, a few round vesicles can be seen near the lip in contact with the cell membrane (Fig. 7 *a*, *arrow*).

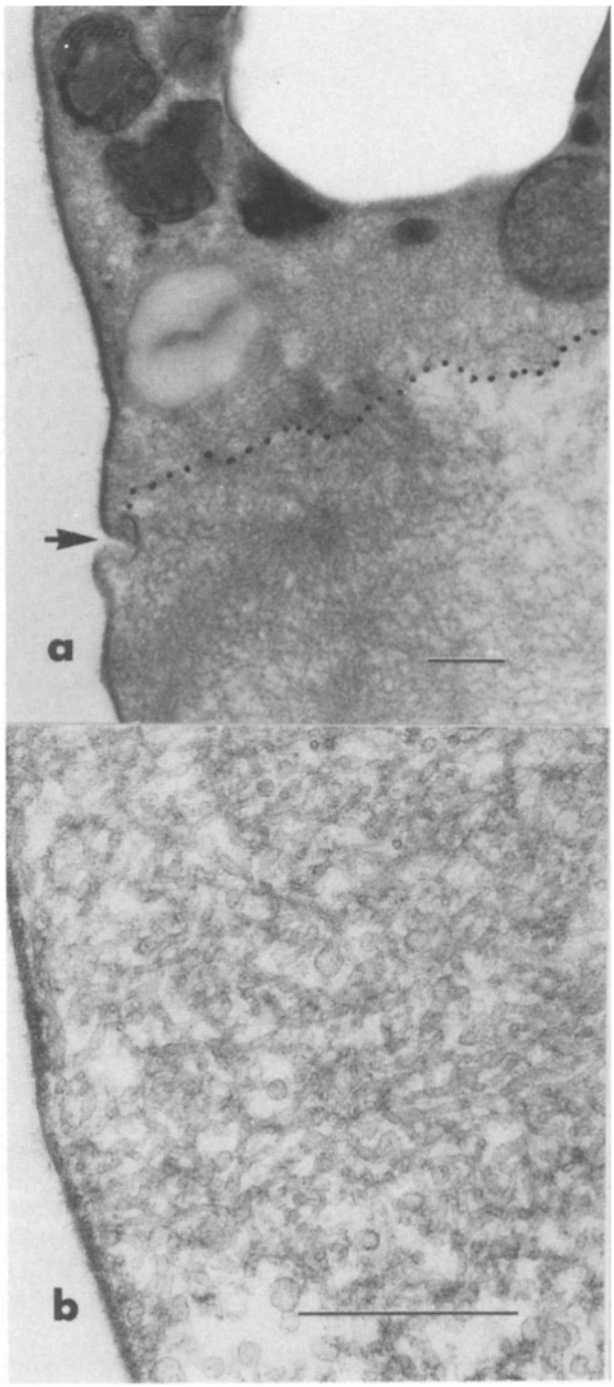

Figure 7. Semithick sections of the pseudopod–cell body junction in glutaraldehyde–tannic acid–saponin fixative. (*a*) A sharp band of densely packed vesicles is seen just within the cell body, often in contact with fiber complexes. The lower margin of the band of vesicles is marked with a dotted line. Many round vesicles appear in contact with the membrane at the lip that marks the lower boundary of the cell body (*arrow*). Other vesicles seem to be dispersed among the filaments of complexes near the junction. (*b*) High magnification micrograph of vesicle region; the band is composed of smooth vesicles with round and tubular profiles. Cortically, the tubular vesicles orient along the pseudopod membrane; internally, they lie parallel to the plane of the junction. Bars, 0.5 μm; V_{accel}, 1 MV.

Immunocytochemistry of the Fiber Complexes

Antibody Characterization. The labeling pattern obtained by probing nitrocellulose blots of the AS-S100 MSP-enriched fraction of sperm homogenate with anti-MSP antibody AZ10 is shown in Fig. 8. The antibody reacts strongly and exclusively with the MSP band which runs at ~15 kD on SDS-polyacrylamide gels.

Labeling Patterns in Fixed, Permeabilized Sperm. Fig. 9 *a* shows that the fiber complexes are visible in unstained sperm fixed in glutaraldehyde–Triton. When incubated with antibody AZ10, filament complexes label heavily by indirect immunofluorescence (Fig. 9 *b*). Complexes in negative-control cells, incubated without first antibody, do not (Fig. 9, *c* and *d*). Some fluorescence found in the cell bodies of both negative controls and anti-MSP-stained cells may be due to autofluorescence of residual glutaraldehyde. The much brighter fluorescence of antibody AZ10–stained cells indicates there is some MSP in the cell bodies of activated cells.

Phalloidin staining was used to determine if the small amount of actin known to exist in *Ascaris* sperm (<0.5% total protein) forms F-actin assemblies in the pseudopod cyto-

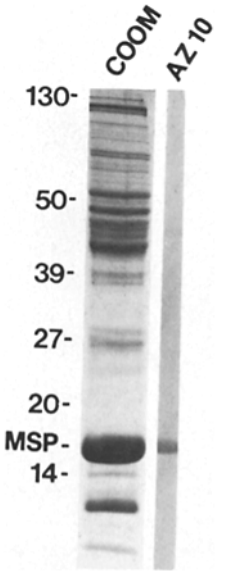

Figure 8. Immunoblot pattern of antibody AZ10 against *Ascaris* sperm protein fraction AS-S100. The left lane (*COOM*) shows the Coomassie Blue–staining pattern of AS-S100 sperm proteins on a 10–20% gradient polyacrylamide gel. MSP is the most abundant protein. The right lane (*AZ10*) is a nitrocellulose immunoblot of *Ascaris* sperm proteins probed with antibody AZ10 followed by horseradish peroxidase–anti-mouse IgG.

skeleton. Fig. 9, *e* and *f*, show that pseudopods of permeabilized spermatozoa fail to label with phalloidin, whereas the mouse peritoneal fibroblast-positive controls show heavy labeling of their actin filament bundles (Fig. 9, *g* and *h*).

At the ultrastructural level (Fig. 10), colloidal gold–labeled antibody AZ10 is shown to decorate the entire fiber complex, including the core as well as individual fibers. Both the preservation of the fibers and permeability to antibody–gold conjugates varied considerably among cells. Fig. 10 *a* shows a thin section through a labeled cell in which the pseudopod remains packed with filaments. Filaments just beneath a disrupted portion of plasma membrane decorate heavily with gold particles, but those within the core of a nearby fiber complex do not. We suspect the nonuniform labeling reflects the failure of gold particles to penetrate areas where filaments are tightly packed, especially at the cores of complexes. In more thoroughly dispersed cells (Fig. 10 *b*), however, some filaments at the core of the fiber complexes were also labeled. Profiles of sperm probed with anti-mouse IgG–gold (Fig. 10 *c*) or BSA–gold (not shown) contained only a few bound gold particles.

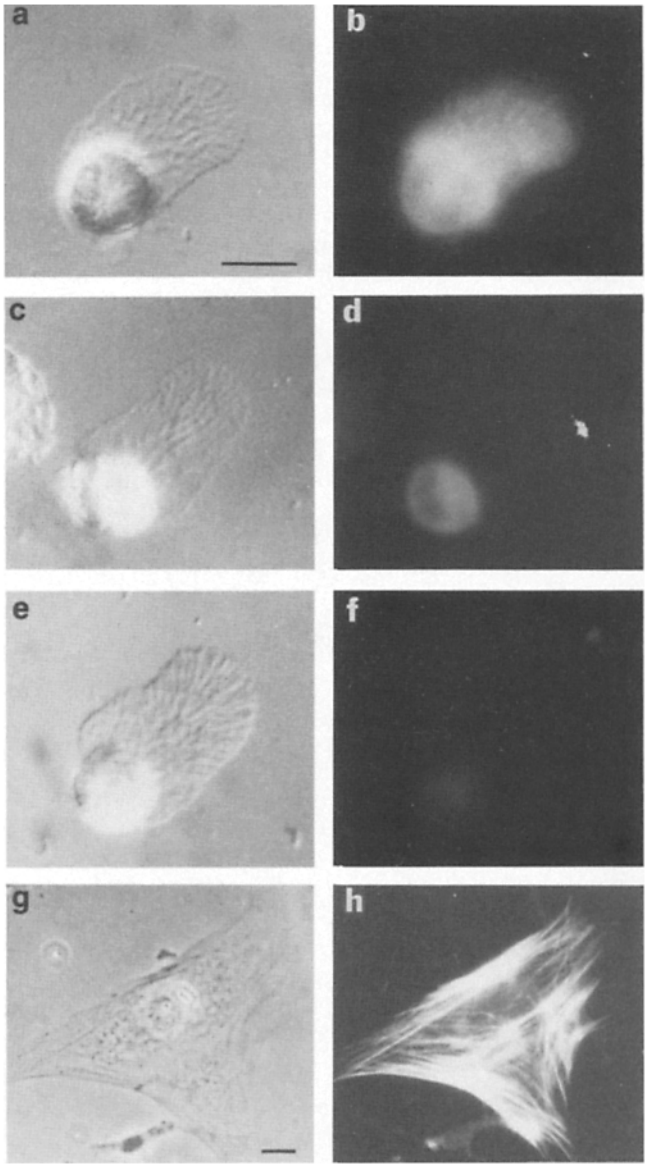

Figure 9. Paired light and fluorescence micrographs of *Ascaris* sperm and mouse peritoneal fibroblasts. (*a* and *b*) *Ascaris* sperm incubated with antibody AZ10 followed by FITC–anti-mouse IgG. The filament complexes are heavily labeled. (*c* and *d*) Control sperm incubated with FITC–anti-mouse IgG only. (*e* and *f*) Sperm labeled with rhodamine-phalloidin. (*g* and *h*) Mouse peritoneal fibroblast incubated with rhodamine-phalloidin showing labeled actin filament bundles. Bars, 10 μm.

Discussion

Summary of Anatomy and Behavior of Ascaris Sperm Cytoskeleton and Pseudopod Membrane Specializations

This work has demonstrated that a coherent, dynamic cytoskeleton exists in the pseudopod of *Ascaris* sperm whose behavior suggests its direct participation in the cell's amoeboid locomotion. The drawing in Fig. 11 summarizes the features of *Ascaris* sperm which have made it an excellent model for studying nematode sperm amoeboid motility: it is relatively large and bipolar with a permanent pseudopod. In sections of cells fixed in situ, all of the membrane-bound organelles (nucleus, mitochondria, membranous organelles, and refractile body) are confined to the cell body; the pseudopod contains fibers. The fibers are organized into superstructures, the fiber complexes, which are visible in living, unstained, unlabeled cells. Radiating fibers from the complexes, shown in the detail, insert into the dense layer of material lining the inside of the pseudopod membrane. The membrane puckers into villipodia as it associates with fibers from the terminations of complexes at the leading edge. The villipodia, the pseudopod's membrane–cytoskeleton unit, appear to be adhesion sites, and spread out as they make contact with substrate or move along, unused, to the cell body where their components are recycled.

Because the fiber complexes can be seen inside the pseudopod of living cells with DIC-light microscopy, the behavior of this system—membrane and cytoskeleton together—can be studied without the ambiguities associated with in-

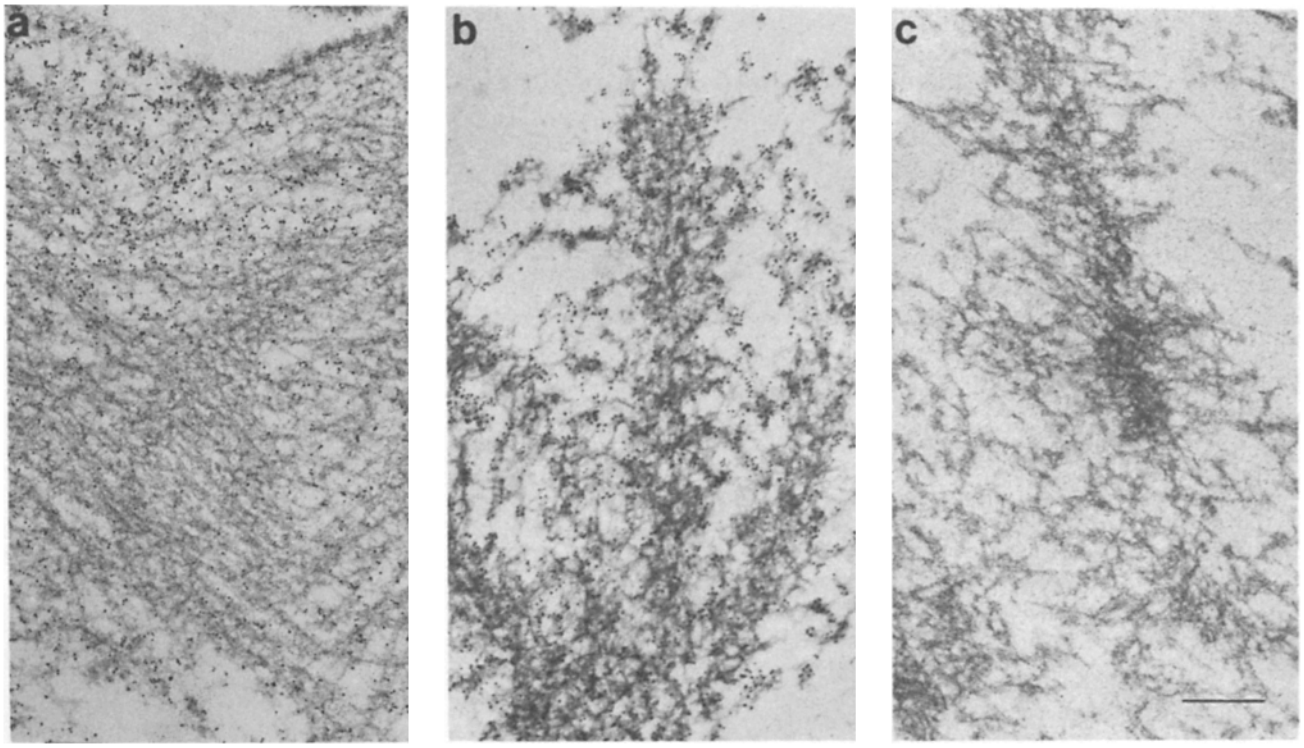

Figure 10. Thin sections of immunogold-labeled *Ascaris* sperm. (*a*) Gold–antibody AZ10–labeled pseudopod with its cytoskeleton largely intact. Filaments beneath the disrupted plasma membrane are heavily decorated; those within the thick mesh of the filament complex in the center are lightly labeled. (*b*) The same antibody–gold labeling of a more dispersed pseudopod cytoskeleton with the cores of the filament complexes exposed; the filaments within are heavily decorated. (*c*) Control cell incubated with gold–anti–mouse IgG alone. Few gold particles are present. Bar, 200 nm; V_{accel}, 80 kV.

direct labeling and bleaching. As shown, the cytoskeleton is being continuously formed at the leading edge of the cell. The membrane specializations and the fiber complexes both move rearwards in unison and both disappear at the junction of pseudopod and cell body. This junction represents a boundary between two very different types of membrane: the highly mobile Triton-extractable pseudopod membrane, and the stable detergent-resistant cell body membrane. (There is also evidence for this difference in the sperm of the nematode *C. elegans*; see below.) In this model, both membrane and

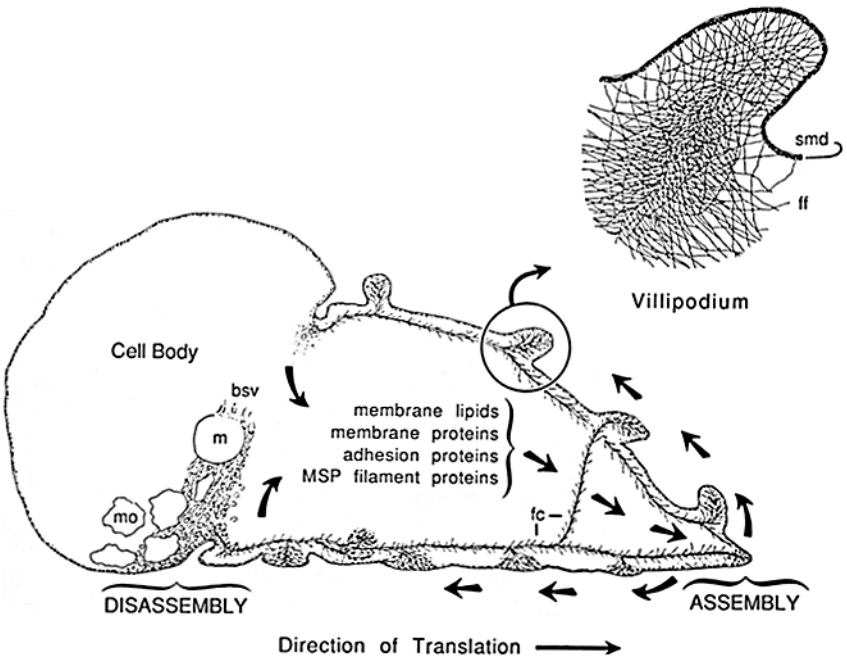

Figure 11. Schematic drawing of membrane and fiber complex movements in pseudopod of crawling *Ascaris* spermatozoon (See text for explanation.).

complexes are assumed to recycle, with the processes of assembly and disassembly being independent and proceeding at the same rate. To crawl, assembly and attachment of membrane and complexes at the tip is required to extend the pseudopod front. As they move rearwards, complexes and their associated villipodia may move either dorsally or ventrally. Disassembly of membrane and complexes at the base is required to pull the cell body forward. This is derived from two observations: (*a*) the pseudopod length remains relatively constant during normal crawling; and (*b*) it can be shown in "aging" crawling cells that even when the assembly of new villipodia at the leading edge of the pseudopod ceases, the cell body continues to be pulled forward (Sepsenwol, S., and S. J. Taft, manuscript submitted for publication). As villipodia reach the base of the pseudopod, it is proposed that pseudopodial membrane and membrane adhesion proteins are internalized and filaments forming the complexes disaggregate (Fig. 11, curved arrows at base of pseudopod). The abundant vesicles at the base of the pseudopod and association of vesicles with the cell membrane is consistent with active endocytosis, but direct evidence is lacking. (See discussion of endocytosis in *C. elegans* below.) Whether the filaments exert force (ie., push or pull) on the attached membrane is not known.

Identification of MSP in the Fiber Complexes of Ascaris Sperm

In the absence of actin, myosins, and/or tubulins in *Ascaris* sperm, the search for new types of cytoskeletal proteins has become central to understanding how this system of locomotion might work. MSP is an obvious candidate for a pseudopod cytoskeletal protein because it is present in the quantity needed to form the mass of filaments that pack the pseudopod. In sperm of both *Ascaris* and *C. elegans*, MSP comprises >15% of the total protein. In *C. elegans*, anti-MSP antibodies had been shown to localize in the pseudopod of activated sperm (Ward and Klass, 1982). Localization at the ultrastructural level, however, has been frustrated by the lack of an identifiable filamentous superstructure in their pseudopods distinguishable from background granular material (Roberts, 1983). The ordered arrangement of filaments in *Ascaris* sperm allows an unequivocal localization of MSP antibodies to the fiber complexes and to the individual filaments that comprise them. This is the first evidence that MSP may be a filament protein in the sperm's pseudopod. This immunocytochemical identification does not preclude the involvement of other proteins in the assembly of fiber complexes. However, the abundance of MSP, its segregation into the pseudopods of motile sperm, and the anti-MSP labeling over all the parts of the complex suggests that it is the major species in this fibrous cytoskeleton. The absence of phalloidin staining indicates that the very low concentration of actin is not in the form of F-actin aggregates in the pseudopod. This result does not exclude copolymerization of whatever actin might be present with other major components of the fibrous cytoskeleton. Indeed, the heterogeneity of fuzzy fibers in *Ascaris* sperm and their unique associations with cell membranes and each other suggests that proteins in addition to MSP may be required to assemble functional fiber complexes.

An antibody generated against *C. elegans* MSP, TR20 (Roberts et al., 1986; Ward et al., 1986), shows the same selectivity for *Ascaris* MSP on Western blots, and stains *Ascaris* sperm fiber complexes in the same pattern as antibody AZ10 (see cover photo). This antibody cross-reactivity confirms molecular studies showing strong similarity between *Ascaris* and *C. elegans* MSP. MSP cDNA's from both species have been cloned and sequenced (Burke and Ward, 1983; Bennett and Ward, 1986) and nucleotide homology is 72%; the predicted proteins both consist of 127 amino acids with 82% homology.

The C. Elegans Spermatozoon: Similarities and Differences

Previous work done on the sperm of the nematode *C. elegans* provides valuable insights into *Ascaris* sperm behavior. Their strong similarities give us reason to believe that they both crawl by the same mechanism. *C. elegans* sperm cells are rich in MSP (see above). Like *Ascaris* sperm, *C. elegans* spermatids can be activated to full motility in vitro (Nelson and Ward, 1980; Ward et al., 1983). The spermatids and activated sperm are three times smaller than *Ascaris* male gametes, but morphologically similar: they show the same permanent compartmentation of organelles. The pseudopod of a crawling *C. elegans* spermatozoon is covered with stubby projections, which form at the tip, move centripetally, and disappear at the pseudopod-cell body junction (see scanning electron micrograph in Nelson et al., 1982, Fig. 1). When attached, these make extensive contacts with the substrate and pull the cell along (Roberts and Streitmatter, 1984). *C. elegans* sperm possess a region of laminar membranes just inside the cell body at its border with the pseudopod, the site of the band of smooth vesicles in *Ascaris* sperm (see Ward et al., 1981; Fig. 4).

Roberts and Ward (1982*a*,*b*) showed that cationic latex beads, ferritin-labeled lectins, and fluorescent-labeled phospholipids all migrated away from the tip of the pseudopod and either accumulated on the surface (beads and lectins) or disappeared (phospholipid) at the pseudopod-cell body junction. Labels over the cell body were stationary in motile sperm. Pavalko and Roberts (1987) have shown that new membrane proteins insert at the tip of the pseudopod and move to the base. The pseudopod labels (colloidal gold and antibody) accumulate at the base. This is direct evidence for incorporation of new membrane proteins at the leading edge of the pseudopod; however, there is as yet no evidence that they are internalized. This lack of direct information about how or whether membrane components are recycled is an important caveat for the *Ascaris* sperm model.

There are differences between these two species of nematode sperm as well. Most importantly, there is no evidence of a higher order fiber structure in the pseudopod of *C. elegans* sperm, even when examined in whole mount and semithick sections with HVEM (for review see Roberts et al., 1989; an exception is the nonmotile *fer-3* sperm mutant, see Ward et al., 1981; Fig. 11, *c* and *d*). The pseudopod is filled entirely with a dense mass of granular material and relatively uniform interconnected 2–3 nm filaments, thought to be polymers of MSP (reviewed in Roberts et al., 1989). It is possible that any filamentous superstructure in *C. elegans* sperm pseudopod might be obscured by the high density of granular cytoplasm. The worms' metabolic systems are also quite different and affect the stability of the pseudopod: *C. elegans* spermatids form pseudopods and crawl under aero-

bic conditions; *Ascaris* sperm require anaerobiosis for activation and locomotion, fully formed cytoskeletons become unstable when the cell is exposed to oxygen. It is not clear if this oxygen toxicity is a direct effect on the *Ascaris* sperm fiber complexes (by peroxide formation, for example) or the consequence of blocking its anaerobic mitochondrial ATP synthesis (for review see Kohler and Bachman, 1980).

Relation of Ascaris Sperm Motility to Other Models for Amoeboid Motility

It would be a mistake to generalize the specialized amoeboid sperm of *Ascaris* into a universal model for all cells that crawl; there are even significant differences among families of nematodes. (The sperm of *Nippostrongylus brasiliensis* creep by means of transverse waves of constriction passing rearwards over their short pseudopods rather than individual villipodia [Wright and Sommerville, 1984]). As a counter example, however, *Ascaris* sperm are useful for testing the heuristic value of some models now proposed for amoeboid locomotion in actin-based cells. For example, two competing models for fibroblast motility are based on bulk membrane flow and discount a direct role for the cytoskeleton in membrane flow (see Ishihara et al., 1988). Bulk membrane flow theory supposes that the retrograde flow of membrane lipids assembled at the leading edge alone generates a motive force and sweeps membrane protein constituents, including adhesion proteins, rearwards (Bretscher, 1983). It is presumed that tethered transmembrane proteins are bound to fixed cytoplasmic elements. After observing the comigration of villipodia and fiber complexes, we have reservations about using bulk membrane flow models to describe *Ascaris* sperm motility. In such a system, in which both membrane and cytoplasmic proteins are moving, it is not clear whether bulk membrane flow is the force or consequence of the continuous assembly and disassembly of the fiber complexes. Regarding the actomyosin-cytoskeleton model, recent reports have demonstrated that myosin I, the most abundant species in amoebae of the slime mold, *Dictyosteleum*, is not absolutely required for crawling (De Lozanne and Spudich, 1987; Knecht and Loomis, 1987). (Interestingly, these data have been cited as evidence for the irrelevance of the cytoskeleton to the engine for crawling [Bretscher, 1988].) While *Ascaris* sperm are neither amoebae nor fibroblasts and do not contain significant actin, their fiber complexes clearly represent a new type of cytoskeleton intimately involved in membrane/cell movement. These kinds of unexpected results should encourage the search for new mechanisms by which cytoskeletal elements such as actin or MSP might participate in amoeboid locomotion.

The authors would like to acknowledge the expert technical assistance of Judith Baumgartner of the University of Wisconsin at Stevens Point and James Pawley of the Madison Integrated Microscopy Resource, and the skillful artwork of Patricia Gasque.

This work was supported in part by National Science Foundation RUI grant DCB8610475, National Institutes of Health (NIH) AREA grant GM-37435-01 to S. Sepsenwol, and NIH grant GM-29994 to T. M. Roberts. The Madison Integrated Microscopy Resource is supported by a grant from the Biomedical Research Technology Program, DRR-NIH P41RR00570.

Received for publication 31 May 1988, and in revised form 13 September 1988.

References

Abbas, M. K., and G. D. Cain. 1984. Amino acid and lipid composition of refringent granules from the ameboid sperm of *Ascaris suum* (Nematoda). *Histochemistry*. 81:59–65.

Bennett, K. L., and S. Ward. 1986. Neither a germ line-specific nor several somatically expressed genes are lost or rearranged during embryonic chromatin diminution in the nematode *Ascaris lumbricoides* var. *suum*. *Dev. Biol.* 118:141–147.

Bretscher, M. S. 1983. Distribution of receptors for transferrin and low density lipoprotein on the surface of giant HeLa cells. *Proc. Natl. Acad. Sci. USA*. 80:454–458.

Bretscher, M. S. 1988. Fibroblasts on the move [review]. *J. Cell Biol.* 106: 235–237.

Burghardt, R. C., and W. E. Foor. 1978. Membrane fusion during spermiogenesis in *Ascaris*. *J. Ultrastruct. Res.* 62:190–202.

Burke, D. J., and S. Ward. 1983. Identification of a large multi-gene family encoding the major sperm protein of *Caenorhabditis elegans*. *J. Mol. Biol.* 171:1–29.

Clarke, M., and J. A. Spudich. 1977. Non-muscle contractile proteins: the role of actin and myosin in cell motility and shape determination. *Annu. Rev. Biochem.* 46:797–822.

De Lozanne, A., and J. A. Spudich. 1987. Disruption of the *Dictyostelium* myosin heavy chain gene by homologous recombination. *Science (Wash. DC)*. 236:1086–1091.

Foor, W. E. 1974. Morphological changes of spermatozoa in the uterus and glandular vas deferens of *Brugia pahangi*. *J. Parasitol.* 60:125–133.

Foor, W. E., M. H. Johnson, and P. C. Beaver. 1971. Morphological changes in the spermatozoa of *Dipetalonema viteae* in utero. *J. Parasitol.* 57:1163–1169.

Ishihara, A., B. Holifield, and K. Jacobson. 1988. Analysis of lateral redistribution of a monoclonal antibody complex plasma membrane glycoprotein which occurs during cell locomotion. *J. Cell Biol.* 106:329–343.

Klass, M., and D. Hirsh. 1981. Sperm isolation and biochemical analysis of the major sperm protein from *Caenorhabditis elegans*. *Dev. Biol.* 84:299–312.

Knecht, D. A., and W. F. Loomis. 1987. Anti-sense RNA inactivation of myosin heavy chain gene expression in *Dictyostelium discoideum*. *Science (Wash. DC)*. 236:1081–1086.

Kohler, P., and R. Bachmann. 1980. Mechanisms of respiration and phosphorylation in *Ascaris* muscle mitochondria. *Mol. Biochem. Parasitol.* 1:75–90.

Laemmli, U. K. 1970. Cleavage of structural proteins during the assembly of the head of bacteriophage T4. *Nature (Lond.)*. 227:680–685.

Maupin, P., and T. D. Pollard. 1983. Improved preservation and staining of HeLa cell actin filaments, clathrin-coated membranes and other cytoplasmic structures by tannic acid-glutaraldehyde-saponin fixation. *J. Cell Biol.* 96: 51–62.

Nelson, G. A., and S. Ward. 1980. Vesicle fusion, pseudopod extension and amoeboid motility are induced in nematode spermatids by the ionophore monensin. *Cell*. 19:457–464.

Nelson, G. A., and S. Ward. 1981. Amoeboid motility and actin in *Ascaris lumbricoides* sperm. *Exp. Cell Res.* 131:149–160.

Nelson, G. A., T. M. Roberts, and S. Ward. 1982. *Caenorhabditis elegans* spermatozoan locomotion: amoeboid movement with almost no actin. *J. Cell Biol.* 92:113–120.

Pavalko, F. M., and T. M. Roberts. 1987. *Caenorhabditis elegans* spermatozoa assemble membrane proteins onto the cell surface at the tips of pseudopodial projections. *Cell Motil. Cytoskeleton*. 7:169–177.

Pawley, J. B., S. Sepsenwol, and H. Ris. 1986. Four-dimensional microscopy of *Ascaris* sperm motility. *Ann. NY Acad. Sci.* 483:171–178.

Pollard, T. D. 1981. Cytoplasmic contractile proteins [review]. *J. Cell Biol.* 91(Pt. 2, Suppl.):156s–165s.

Pollard, T. D. 1986. Assembly and dynamics of the actin filament system of non-muscle cells. *J. Cell Biochem.* 31:87–95.

Ris, H. 1985. The cytoplasmic filament system in critical point-dried whole mounts and plastic-embedded sections. *J. Cell Biol.* 100:1474–1487.

Roberts, T. M. 1983. Crawling *Caenorhabditis elegans* spermatozoa contact the substrate only by their pseudopods and contain 2-nm filaments. *Cell Motil. Cytoskeleton*. 8:130–142.

Roberts, T. M., and G. Streitmatter. 1984. Membrane–substrate contact under the spermatozoon of *Caenorhabditis elegans*, a crawling cell that lacks filamentous actin. *J. Cell Sci.* 69:117–126.

Roberts, T. M., and S. Ward. 1982*a*. Centripetal flow of pseudopodial surface components could propel the amoeboid movement of *Caenorhabditis elegans* spermatozoa. *J. Cell Biol.* 92:132–138.

Roberts, T. M., and S. Ward. 1982*b*. Membrane flow during nematode spermiogenesis. *J. Cell Biol.* 92:113–120.

Roberts, T. M., F. M. Pavalko, and S. Ward. 1986. Membrane and cytoplasmic proteins are transported in the same organelle complex during nematode spermatogenesis. *J. Cell Biol.* 102:1787–1796.

Roberts, T. M., S. Sepsenwol, and H. Ris. 1989. Sperm motility in nematodes: crawling movement without actin. *In* The Cell Biology of Fertilization. H. Schatten and G. Schatten, editors. Academic Press, Orlando, FL. 41–60.

Sepsenwol, S., T. Braun, and M. Nguyen. 1986. Adenylate cyclase activity is

absent in inactive and motile sperm in the nematode parasite, *Ascaris suum*. *J. Parasitol.* 72:962–964.

Slot, J. W., and H. J. Geuze. 1985. A new method of preparing gold probes for multiple labelling cytochemistry. *Eur. J. Cell Biol.* 38:87–93.

Towbin, H., T. Staehelin, and G. Gordon. 1979. Electrophoretic transfer of proteins from polyacrylamide gels to nitrocellulose sheets: procedure and some applications. *Proc. Natl. Acad. Sci. USA.* 76:1350–1354.

Trinkhaus, J. P. 1984. Cells into organs. *In* The Forces That Shape the Embryo. 2nd edition. Prentice-Hall, Englewood Cliffs, NJ. 541 pp.

Ward, S., and M. Klass. 1982. The localization of the major sperm protein in *C. elegans* sperm and spermatocytes. *Dev. Biol.* 92:203–208.

Ward, S., Y. Argon, and G. A. Nelson. 1981. Sperm morphology in wild-type and fertilization-defective mutants of *Caenorhabditis elegans*. *J. Cell Biol.* 91:26–44.

Ward, S., E. Hogan, and G. A. Nelson. 1983. The initiation of *Caenorhabditis elegans* spermiogenesis *in vivo* and *in vitro*. *Dev. Biol.* 98:70–79.

Ward, S., T. M. Roberts, S. Strome, F. M. Pavalko, and E. Hogan. 1986. Monoclonal antibodies that recognize a polypeptide antigenic determinant shared by multiple *Caenorhabditis elegans* sperm-specific proteins. *J. Cell Biol.* 102:1778–1786.

Wright, E. J., and R. I. Sommerville. 1984. Postinsemination changes in the amoeboid sperm of a nematode, *Nippostrongylus brasiliensis*. *Gamete Res.* 10:397–413.

Wright, E. J., and R. I. Sommerville. 1985. Structure and development of the spermatozoon of the parasitic nematode, *Nematospiroides dubius*. *Parasitology*. 90:179–192.